JOURNAL OF GEOPHYSICAL RESEARCH, VOL. 101, NO. B11, PAGES 25,459–25,471, NOVEMBER 10, 1996

# The 1954 Rainbow Mountain-Fairview Peak-Dixie Valley earthquakes: A triggered normal faulting sequence

Kathleen M. Hodgkinson and Ross S. Stein
U.S. Geological Survey, Menlo Park, California

Geoffrey C. P. King
Institut de Physique du Globe de Paris, France

**Abstract.** In 1954, four earthquakes of $M > 6.0$ occurred within a 30 km radius in a period of six months. The Rainbow Mountain-Fairview Peak-Dixie Valley earthquakes are among the largest to have been recorded geodetically in the Basin and Range province. The Fairview Peak earthquake ($M$=7.2, December 12, 1954) followed two events in the Rainbow Mountains ($M$=6.2, July 6, and $M$=6.5, August 24, 1954) by 6 months. Four minutes later the Dixie Valley fault ruptured ($M$=6.7, December 12, 1954). The changes in static stresses caused by the events are calculated using the Coulomb-Navier failure criterion and assuming uniform slip on rectangular dislocations embedded in an elastic half-space. Coulomb stress changes are resolved on optimally oriented faults and on each of the faults that ruptured in the chain of events. These calculations show that each earthquake in the Rainbow Mountain-Fairview Peak-Dixie Valley sequence was preceded by a static stress change that encouraged failure. The magnitude of the stress increases transferred from one earthquake to another ranged from 0.01 MPa (0.1 bar) to over 0.1 MPa (1 bar). Stresses were reduced by up to 0.1 MPa over most of the Rainbow Mountain-Fairview Peak area as a result of the earthquake sequence.

## Introduction

The 1954 Rainbow Mountain-Fairview Peak-Dixie Valley earthquakes occurred within the Central Nevada Seismic Zone, a band of seismicity which trends north-northeast through central Nevada. The sequence involved four earthquakes of $M \geq 6.0$ that occurred within a 30 km radius and in a period of 6 months (Figure 1). The series began with two oblique-slip events on the Rainbow Mountain fault, July 6, 1954 ($M$=6.2) and August 24, 1954 ($M$=6.5). On December 16, 1954, an $M$=7.2 oblique slip event occurred on the Fairview Peak fault [*Doser,* 1986]. The West Gate and Gold King faults ruptured with the Fairview Peak earthquake. Four minutes and twenty seconds later, the Dixie Valley fault ruptured ($M$=6.7). Surface ruptures indicate this was a normal faulting event. These earthquakes are among the largest to have been recorded geodetically and seismically in the Basin and Range province. *Wallace* [1984] reported that the faults that ruptured in the 1954 events had not previously ruptured in at least 300, if not thousands of years, and that the events were part of a 100-year period of heightened activity in the Central Nevada Seismic Zone. Fifteen earthquakes of $M_S$>5.5 occurred within the seismic zone between 1915 and 1954 [*Doser,* 1988]. In the Walker Lane zone, a northwest trending shear zone of right-lateral faults which extends from southeast to western Nevada, six events of $M_S$>5.5 occurred between 1932 and 1959 (Figure 2) [*Doser,* 1988].

It has been proposed that earthquake generated increases in the static stress field can induce an increase in seismicity rates and trigger moderate to large earthquakes [*Harris and Simpson,* 1992; *Jaumé and Sykes,* 1992; *Stein et al.,* 1992; *Reasenberg and Simpson,* 1992; *Simpson and Reasenberg,* 1994; *King et al.,* 1994]. By this theory, each earthquake releases stress on the fault that slips but transfers the stress elsewhere. The rate of subsequent earthquakes is then higher where stress is raised. Nonelastic effects such as the postseismic redistribution of stress must also affect the rate and distribution of subsequent earthquakes and are not included in this analysis. The reasonable agreement, however, between seismicity and changes in the static stress field suggest that a simple elastic analysis captures much of the nature of earthquake distribution in the decades following the initial event [*Reasenberg and Simpson*, 1992; *King et al.*, 1994; *Harris et al.,* 1995; *Harris and Simpson,* 1996]. By calculating the static stress changes associated with each earthquake in the 1954 sequence we determine whether the stress changes caused by each event encouraged or discouraged the succeeding events.

## Method

### The Coulomb Failure Criterion

When calculating Coulomb static stress changes, it is assumed that fault failure occurs when the shear and normal stresses on the fault satisfy the Navier-Coulomb failure criterion which is expressed as



Paper number 96JB01302.
0148-0227/96/96JB-01302$09.00

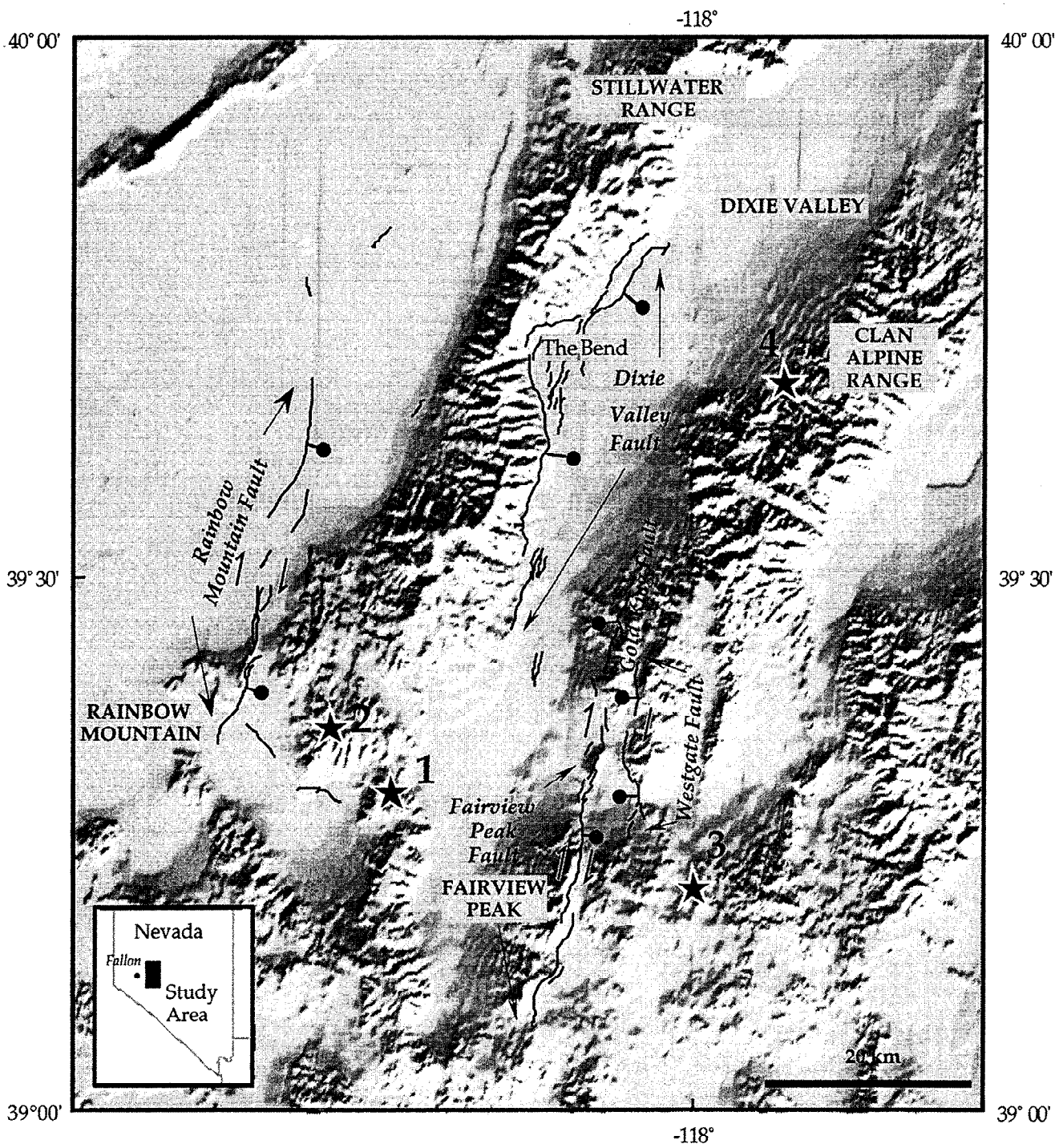


**Figure 1.** Epicenters (stars) and order of the 1954 earthquakes [*Doser*, 1986]. The faults models used in this study were derived from geodetic and geologic observations. Earthquakes are numbered in the order which they occurred: 1 Rainbow Mountain, July 6, $M$=6.2; 2 Rainbow Mountain, August 24, $M$=6.5; 3 Fairview Peak, December 16, $M$=7.2; and 4 Dixie Valley, December 16, $M$=6.7. Inset shows location of the study area. Fault ruptures are shown as thin black lines.

$$\tau_s = S_o + \mu\sigma_n, \tag{1}$$

where $\mu$ is the coefficient of friction, $\sigma_n$ is the normal stress, $\tau_s$ is the shear stress and $S_o$ is the cohesion of the rock. Fluid in a fault zone reduces the normal stresses by an amount equal to the pore pressure. Thus an increase in pore pressure $P$ reduces the normal stress resulting in a weaker fault. Following *Simpson and Reasenberg* [1992], the Coulomb-Navier failure criterion then becomes

$$\tau_s = S_o + \mu(\sigma_n - P). \tag{2}$$

where positive $\sigma_n$ indicates compression. Failure on the fault plane will occur when

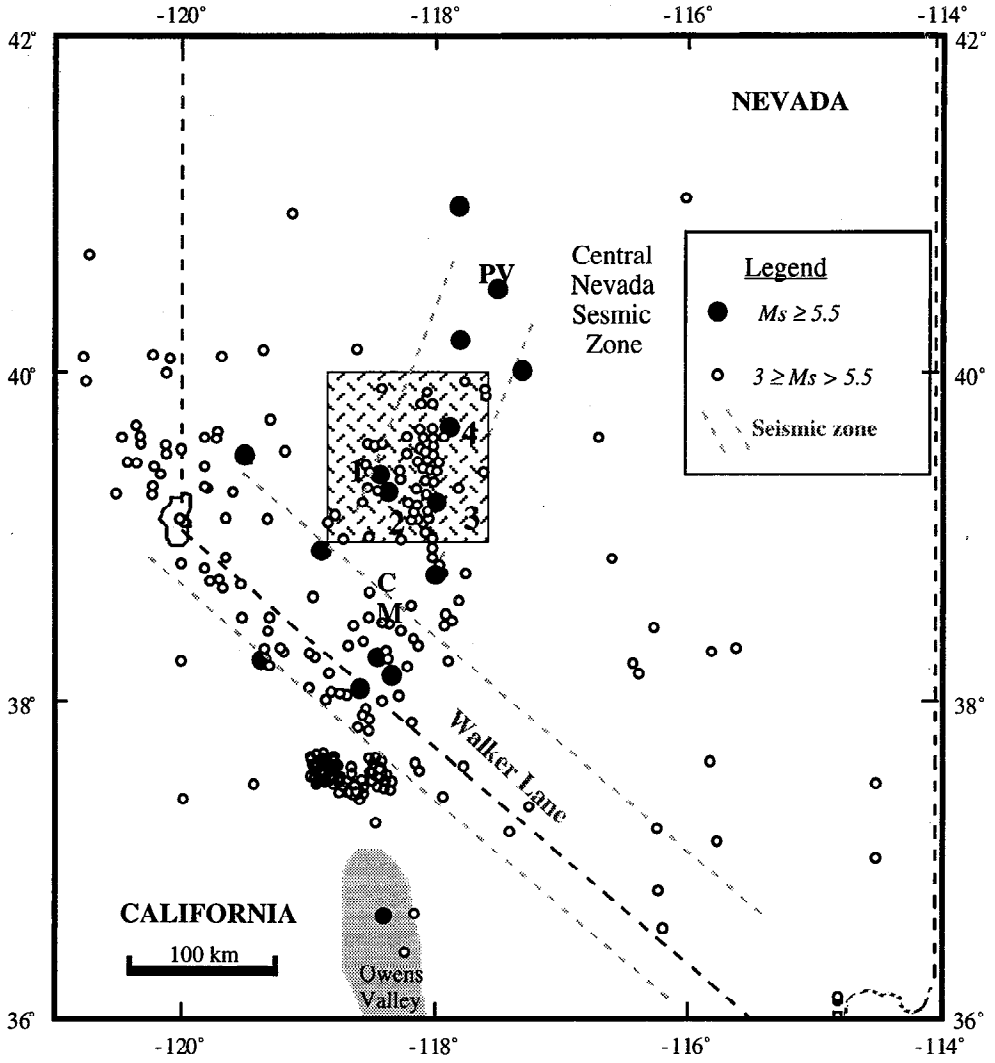


**Figure 2.** Historical seismicity within the western Basin and Range province. Rectangle shows the Rainbow Mountain-Fairview Peak-Dixie Valley study area. The shaded area is Owens Valley. Earthquakes along the eastern margin of the Basin and Range province since 1857 of M ≥ 3 are shown as open circles. Earthquakes greater than M ≥ 5.5 are shown as solid circles. Stippled area shows the study area. Earthquakes are, 1, Rainbow Mountain; 2, Rainbow Mountain; 3, Fairview Peak; 4, Dixie Valley; CM, 1932 Cedar Mountain M=6.7; PV, 1915 Pleasant Valley, M=6.9.

$$\tau_s - S_o - \mu(\sigma_n - P) > 0. \quad (3)$$

If the failure plane is oriented at an angle $\theta$ to the axes of the principal stresses $\sigma_1$ and $\sigma_3$, then equation (2) is written as

$$\sigma_f = \frac{1}{2}(\sigma_1 - \sigma_3)(\sin 2\theta - \mu\cos 2\theta) - \frac{1}{2}\mu(\sigma_1 + \sigma_3) + \mu P - S_o \quad (4)$$

where $\sigma_f$ is the static failure stress [*King et al.*, 1994].

### Static Stress Change Calculation

The coseismic static failure stress change on a fault plane, $\Delta\sigma_f$, is equal to the change between preseismic and postseismic static stresses. If it is assumed that the coefficient of friction, $\mu$, and the cohesion of the rock, $S_o$, remain constant, then

$$\Delta\sigma_f = \Delta\tau_s - \mu(\Delta\sigma_n - \Delta P), \quad (5)$$

where $\Delta\tau_s$ is the change in shear stress, $\Delta\sigma_n$ is the change in normal stress, and $\Delta P$ is the change in pore pressure [*Harris and Simpson*, 1992; *Stein et al.*, 1992; *King et al.*, 1994; *Simpson and Reasenberg*, 1994]. The change in pore pressure $\Delta P$ can be defined in terms of Skempton's coefficient $B$, which can vary from 0 to 1 [*Roeloffs*, 1988], and the mean normal stress, i.e.,

$$\Delta P = -B\frac{\Delta\sigma_{kk}}{3} \quad (6)$$

where

$$\sigma_{kk} = \sigma_{11} + \sigma_{22} + \sigma_{33}$$

[*Simpson and Reasenberg*, 1994]. In the fault zone the normal stresses $\sigma_{11}$, $\sigma_{22}$, and $\sigma_{33}$ are approximately equal. The mean

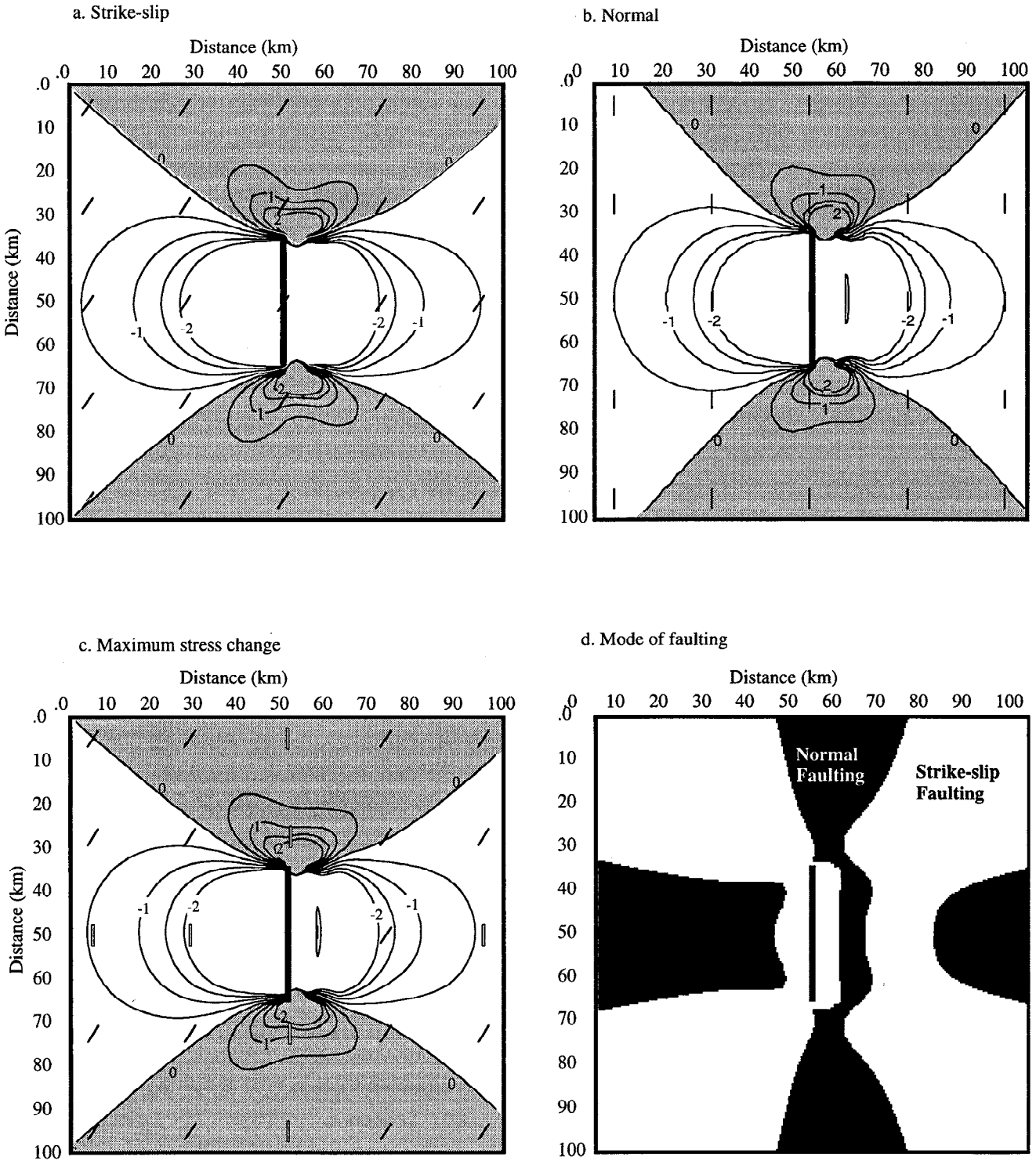


**Figure 3.** Coulomb stress changes associated with 1 m of normal slip on a 60°E dipping fault. The stress changes are contoured at $0.5 \times 10^5$ Pa intervals. The regional stresses are that of east-west extension. (a) Stress changes encouraging strike-slip failure. Small black lines indicate the strike of planes which are most likely to fail through right-lateral slip. (b) Stress changes encouraging normal failure. The strike of optimally dipping faults is north-south. (c) The maximum Coulomb stress change field. The orientations of optimally oriented vertical faults are shown as black lines, and optimally oriented normal faults are shown as white lines. (d) The difference between stress changes encouraging normal faulting and strike-slip faulting. Areas where stress changes encouraging normal faulting are white, while areas where stress changes encouraging strike-slip faulting is greatest are black.

normal stress is therefore $\approx \sigma_{kk}/3$ [*Rice*, 1992]. Thus

$$\Delta P = -B\Delta\sigma_n.$$

The change in stress can then be written as

$$\Delta\sigma_f = \Delta\tau_s - \mu'(\Delta\sigma_n), \tag{7}$$

where $\mu' = \mu(1-B)$ is the apparent coefficient of friction. A positive $\Delta\sigma_f$ indicates that the fault has been brought closer to failure. A negative $\Delta\sigma_f$ indicates a stress decrease and a lowered likelihood of fault failure. The Coulomb static stresses are calculated by assuming uniform slip on rectangular dislocations embedded in an elastic half-space [*Okada*, 1992].

We calculate the static stress change both in the direction of slip on the faults that ruptured, and on planes which are optimally oriented for failure, i.e., those fault orientations on which the Coulomb stress change is maximized [*King et al.*, 1994]. We do this because calculating the stress change on optimally oriented faults has proved successful in determining regions where aftershocks are likely to occur (e.g., *King et al.*, 1994; *Stein et al.*, 1992; *Stein and Lisowski*, 1983]. Coulomb stress changes are resolved onto optimally oriented vertical faults and optimally dipping normal faults. In the case of optimally oriented vertical faults, vertical planes are identified on which the static stress changes encouraging right-lateral slip are maximized. In the case of optimally oriented dipping faults, dipping planes are identified on which the static stress changes encouraging normal slip are maximized. The dip of optimally dipping faults and the strike of optimally striking vertical faults are dependent on $\mu$ and the orientation of the principal stresses which is calculated from the sum of the regional stress and coseismic stress change. The axes of greatest and least compression are given by

$$\Psi = \frac{1}{2}\tan^{-1}\left(\frac{2\sigma^t_{xy}}{\sigma^t_{xx} - \sigma^t_{yy}}\right), \tag{8}$$

where $\sigma^t$ signifies the total stress, coseismic plus regional [*King et al.*, 1994; *Turcotte and Schubert*, 1982]. The angle $\theta$ is the orientation of a fault on which the Coulomb stress change is greatest and is found by differentiating (4) with respect to $\theta$ which yields

$$\tan 2\theta = \pm\frac{1}{\mu}. \tag{9}$$

(Note that equation (9) is given incorrectly by *King et al.'s*, [1994] equation (5)). Optimally dipping normal faults strike perpendicular to the axis of minimum principal stress; their dip is given by $\Psi \pm \theta$. The strike of the optimally oriented vertical faults is given by $\Psi \pm \theta$. The stress change on optimally oriented faults may then be calculated by substituting the corresponding values of shear and normal stresses into equation (7).

As an example, the static stress changes induced by 1 m of normal slip on a 30-km-long, 10-km-deep, 60°E dipping fault are illustrated in Figure 3. A coefficient of friction of 0.4, a Skempton's coefficient of 0, and an east-west extensional regional stress of $10^7$ MPa, are assumed. The Coulomb stress changes are calculated at depths of 5 km on optimally oriented vertical faults (Figure 3a), and optimally oriented normal faults (Figure 3b). The two stress fields are similar; both optimally oriented strike-slip faults and normal faults to the east and west of the slipped fault are relaxed. The strike of optimally dipping normal faults is north-south, perpendicular to the direction of extension. The strike of optimally oriented vertical faults is ~N34°E or N34°W. Only at the end points of the fault are stresses increased. The maximum of either of these two fields gives the field of maximum stress change in the region (Figure 3c). This quantity shall be called the maximum Coulomb stress change, and it shows where triggered events are most likely to occur as a result of increases in the static stress field. The difference between the increase of stress encouraging normal slip and the increase encouraging right-lateral slip suggests which mechanism may dominate; this is illustrated in Figure 3d.

## Modeling the 1954 Earthquake Sequence

The static stress changes caused by each earthquake in the sequence were calculated in three stages: (1) stress caused by slip on the Rainbow Mountain fault only, (2) stress caused by slip on the Rainbow Mountain, Fairview Peak and West Gate/Gold King faults, and (3) stress changes caused by slip on all faults. The fault geometries of each of the faults which ruptured and the associated coseismic slip values were

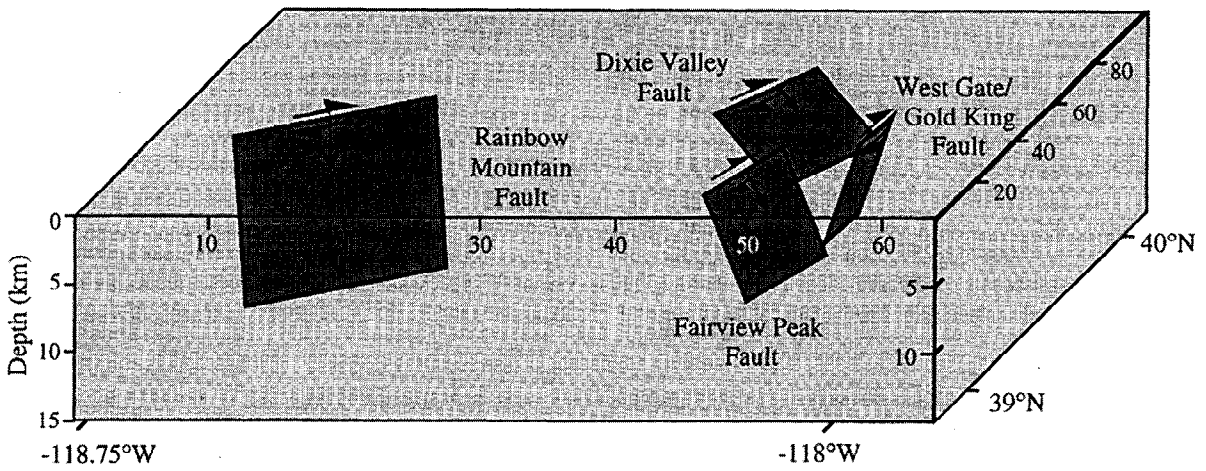


**Figure 4.** The spatial distribution of the faults modeled.

**Table 1.** Fault Geometries for the Rainbow Mountain, Fairview Peak, Fairview Peak South, West Gate/Gold King and Dixie Valley Faults Used in Stress Modeling

| Parameter | Rainbow Mountain | Fairview Peak | Fairview Peak South | West Gate/ Gold King | Dixie Valley |
|---|---|---|---|---|---|
| Dip | 87°E | 69.0°E | 64.0°E | 81°W | 49.0°E |
| Depth, km | 14.0 | 8.0 | 8.0 | 8.0 | 5.5 |
| Strike | N25°E | N4°E | N4°W | N0°E | N8°E |
| Length, km | 24.90 | 24.16 | 13.20 | 16.00 | 24.30 |
| Strike-slip, m | 0.91 | 3.30 | 0.20 | 3.35 | 2.00 |
| Vertical-slip, m | 0.21 | 1.80 | 1.15 | 1.60 | 3.70 |

Fault geometries and slip estimates were derived from an inversion of coseismic geodetic data.

determined from an inversion of coseismic geodetic data [*Hodgkinson et al., this issue*]. The system of faults that best fit the geodetic data was used to model the stress changes. This included a 13-km fault to the south end of the Fairview Peak fault, called the Fairview Peak South fault. Since it was not possible to distinguish between slip on the West Gate and Gold King faults, these two faults were modeled as one fault. Figure 4 shows the spatial distribution of the faults at the surface, and Table 1 shows the coseismic slip values used.

The parameters which define the stress changes on optimally oriented faults are the magnitude and orientation of the regional stress field and the apparent coefficient of friction $\mu'$. Stress changes on optimally oriented faults are not very sensitive to the magnitude of the regional stress field, but they are sensitive to its orientation [*King et al.*, 1994]. The Basin and Range Province is a region of widescale extensional tectonics. The principal stresses are oriented approximately in the vertical and horizontal planes [*Zoback*, 1989]. The axis of minimum compressive stress, $\sigma_3$, varies from east-west along the Sierra Nevada boundary to N60°W in active interior parts of the province such as the Dixie Valley region [*Zoback*, 1989]. This orientation is derived from fault slip data sets, hydrofractures, and earthquake focal mechanisms [*Zoback*, 1989]. Repeated measurements of a trilateration network in the Fairview and Dixie Valley area between 1973 and 1994 yielded a principal extensional strain axis oriented at N61°W±3.8° [*Savage et al.*, 1995]. The central point of the Fairview geodetic network is situated on Fairview Peak, and the network is ideally placed to monitor strain within the 1954 rupture zone. The principal axis of extension determined geodetically agrees well with the independent data sets studied by *Zoback* [1989]. Thus, in calculating the stress change on optimally oriented faults we assume the principal axis of maximum extension to be oriented at N60°W. The magnitude of the stress field is nominally set to 10 MPa.

*King et al.* [1994] showed that the Coulomb stress changes on optimally oriented faults were not greatly changed when $\mu'$ was increased from 0 to 0.75. Low stress drops associated with earthquakes and the lack of high heat flow in fault zones such as the San Andreas suggest that below the upper few kilometers of the brittle crust the value of $\mu$ is lower than 0.6. The best correlation of seismicity rate changes and Coulomb stress changes south of the San Francisco Bay area following the Loma Prieta event were obtained using $\mu' = 0.2$, and a good agreement between Landers aftershock locations and the Coulomb stress increase was found using an apparent coefficient of friction of 0.2 by *Reasenberg and Simpson* (1994) and 0.4 by *King et al.* (1994). Hence an apparent coefficient of friction of 0.4 was used to model the static stress changes on optimally oriented faults. Stress changes in the direction of slip on the faults are calculated using apparent coefficients of friction of 0, which would imply a very weak fault, 0.4, and 0.75, which would imply a very strong fault. The calculation is independent of the regional stress field and depends only on the apparent coefficient of friction. In all calculations a Skempton's coefficient of 0 is assumed.

## Results

### Stress Changes Preceding the Fairview Peak Earthquake

Static stress changes encouraging right-lateral slip on the Fairview Peak fault caused by the Rainbow Mountain events are at most $0.2 \times 10^5$ Pa (0.2 bars), assuming $\mu'=0.4$, and decrease with increasing friction (Figure 5a, and Table 2). The Coulomb stress changes at depths of 7 km are shown since this is the base of the faults as determined geodetically [*Hodgkinson et al.*, 1996]. The stress changes become negative at 5 km along the fault. Stress changes encouraging normal faulting are at most $0.04 \times 10^5$ Pa and are approximately the same for all values of $\mu'$. The West Gate/Gold King fault received the largest increases in static stress from the Rainbow Mountain events. Right-lateral strike-slip faulting was encouraged by a stress changes of up to $0.65 \times 10^5$ Pa, for $\mu'=0.4$, and normal faulting was encouraged by a stress change of $0.7 \times 10^5$ Pa (Figure 5b). Normal and right-lateral stresses resolved onto the Dixie Valley fault were ~3 times greater that those on the Fairview Peak fault (Figure 5c). The stress changes encouraging right-lateral and normal slip were up to $0.7 \times 10^5$ Pa and $0.1 \times 10^5$ Pa, respectively. Almost the entire Dixie Valley fault was brought closer to normal failure (for $\mu'=0.4$), while stress changes encouraging right-lateral failure were positive only along the southern half of the fault.

Planes that were optimally oriented for normal failure in the Dixie Valley-Fairview Peak region were oriented northeast-southwest, close to the orientations of the faults that failed (Figure 6). Stress changes on favorably oriented planes around the Fairview Peak fault were at most $0.15 \times 10^5$ Pa and were positive only at the north end of the fault. There was little variation in stress change with depth (Figure 7). Increasing the apparent coefficient of friction decreased the calculated stress changes on optimally oriented faults near the Fairview Peak fault. Values of $\mu'=0.2$ to $\mu'=0.8$ ($B=0$), resulted in stress changes on the fault varying from 0.3 to $0.1 \times 10^5$ Pa, respectively. The stress changes encouraging normal faulting were greater than those encouraging strike-slip faulting along the Fairview fault (Figure 6b). Stress changes on the West Gate/Gold King fault encouraging normal faulting and strike-

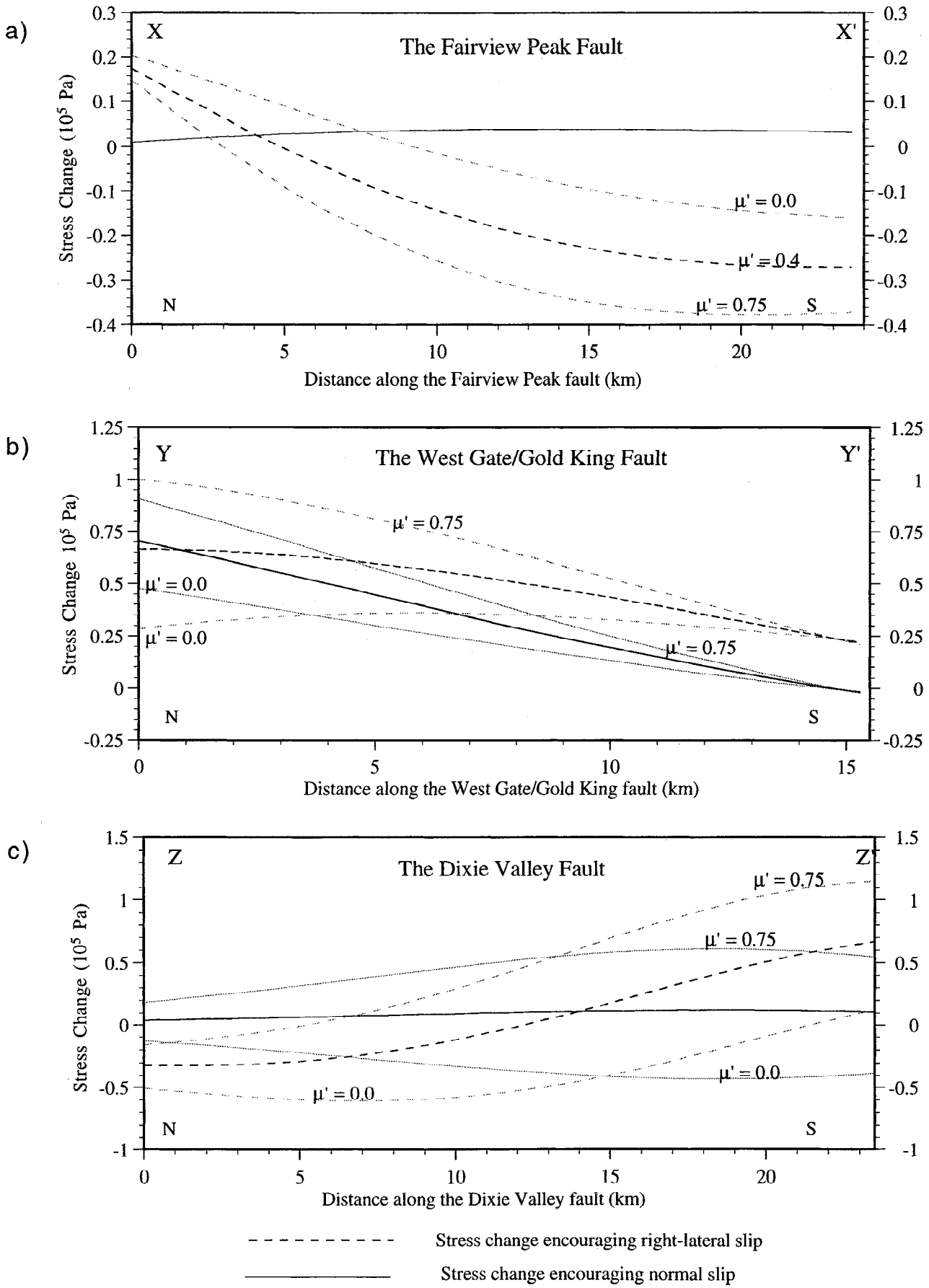


**Figure 5.** Stresses induced by the Rainbow Mountain event resolved onto (a) the Fairview Peak fault, (b) the West Gate/Gold King fault, and (c) the Dixie Valley fault. Calculations are made for μ'=0.0, 0.4 and 0.74. The solid lines represent calculations made with μ'=0.4 and the shaded line represent the upper and lower limits of these values calculated using μ'=0.0 and 0.75. For positions XX', YY', and ZZ', see Figure 6a.

**Table 2.** Stress-Change Induced by Each Event in the 1954 Earthquake Sequence

| Triggering Earthquakes | | Triggered Earthquakes | Calculated Stress Change,* ($x10^5$ Pa) | | |
|---|---|---|---|---|---|
| | | | Resolved | | Optimally - Orientated |
| | | | Right-Lateral | Normal | N60°W |
| RM | → | F | 0.20 | 0.04 | 0.1 |
| | | WG/GK | 0.65 | 0.70 | 0.6 |
| | | DV | 0.70 | 0.12 | 1.0 |
| RM+FP+WG | → | DV | 3.00 | 0.40 | 1.0 |

The stress- changes on optimally oriented faults and those resolved in the direction of slip on each fault are shown. RM, Rainbow Mountain fault; F, Fairview fault; WG/GK, West Gate/Gold King fault; DV, Dixie Valley fault).
*Assumed μ=0.4. Maximum stress change at 7 km shown.

slip faulting stress were up to $1x10^5$ Pa. The Dixie Valley fault received a relatively large stress increase, greater than $1x10^5$Pa, on both the right-lateral and normal-faulting optimally oriented faults. The stress changes encouraging normal faulting, however, were greater than those encouraging right-lateral faulting (Figures 6b).

### Stress Change Preceding the Dixie Valley Event

The combined stress changes resulting from the Rainbow Mountain, Fairview Peak, West Gate and Gold King events encouraged normal faulting along the northern half of the fault where the Dixie Valley epicenter was located [*Doser,* 1986]. The stress changes encouraging right-lateral faulting were large, up to $3x10^5$ Pa for an apparent coefficient of friction of 0.4 (Figure 8). Stress changes encouraging normal faulting were small and varied from $4x10^5$ Pa for $\mu'$=0.75 to $-4x10^5$ Pa for $\mu'$=0.0. For $\mu'$=0.4 the fault received between 0.1 and $0.4x10^5$ Pa of stress increase encouraging normal failure. Toward the southern end of the fault, where rupture ceased, the stress changes were negative, up to $-20x10^5$ Pa.

The Rainbow Mountain, Fairview Peak, and West Gate/Gold King earthquakes created a region of increased static stresses within Dixie Valley. The stress changes on optimally oriented faults along the future rupture zone of the Dixie Valley earthquake were greater than $1x10^5$ Pa along

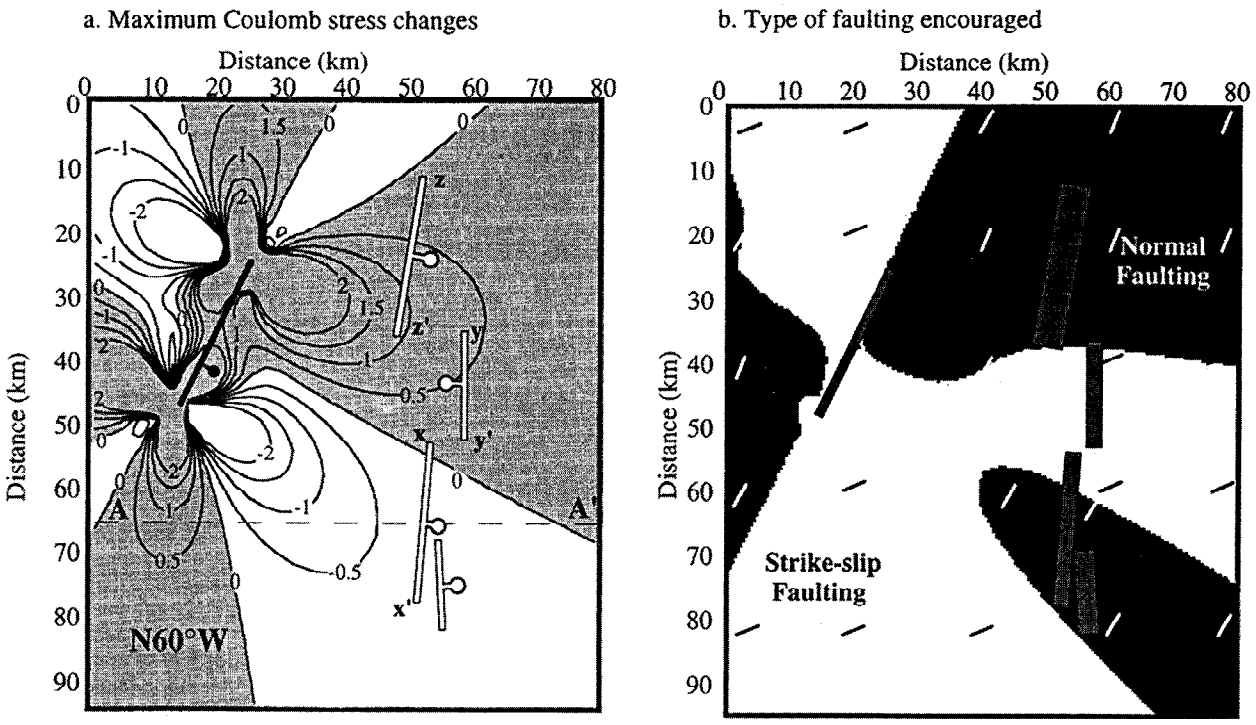


**Figure 6.** Coulomb stress change fields associated with slip on the Rainbow Mountain fault. Friction coefficient μ = 0.4. Depth is 7 km. (a) The maximum Coulomb stress change. The stress changes are contoured at $0.5x10^5$ Pa intervals. Faults in black indicate those that have slipped, while those in white indicate those that have yet to slip. (b) Type of faulting encouraged. Black areas show where stress changes encouraging normal faulting are greater than those encouraging strike-slip faulting. White areas show where stress changes encouraging strike-slip faulting were greatest. Small black lines show the strike of optimally oriented strike-slip faults, and the white lines show the strike of optimally oriented normal faults. Surface projections of faults are shown in Figure 6b.

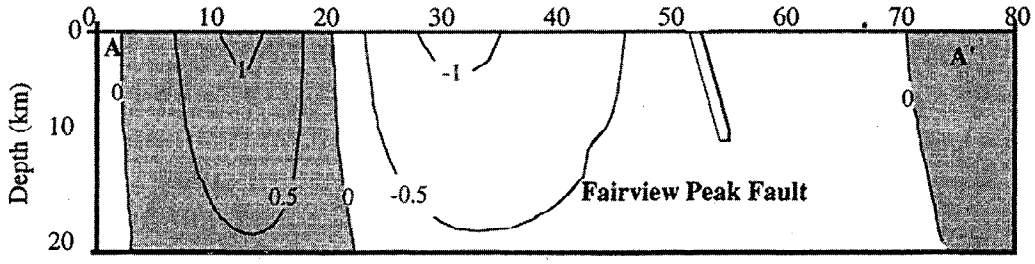


**Figure 7.** Coulomb stress changes across the Dixie Valley fault caused by slip on the Rainbow Mountain fault along profile AA' (shown in Figure 6a). The stress changes are contoured at $0.5 \times 10^5$ Pa intervals.

70% of the fault (Figure 9a). Within the valley and along the eastern side of the Stillwater Mountain Range, stress changes encouraging strike-slip faulting were greatest. At depths of 10 to 12 km, where the hypocenter was located [*Doser*, 1986], the stress increases were about $1 \times 10^5$ Pa (Figure 10).

### Stress Change Resulting From Slip on All Faults in the Sequence

There is a positive though imperfect correlation between areas of positive Coulomb stress change caused by the 1954 earthquake sequence and seismicity in the area between 1955 and 1991 (Plate 1). Red areas indicate regions that received a positive Coulomb stress change and regions where seismicity in following years would be expected to occur. Seismicity is concentrated in a north-south band along the Fairview Peak, West Gate, and Dixie Valley ruptures as are the positive stress changes. The seismicity though is more diffuse than the 5- to 10-km-wide bands of positive stress changes would predict. There are few events to the west of the Rainbow Mountain fault where the Coulomb stress increases are negative, and the seismicity around the southwest of the Fairview Peak fault and to the east of the Dixie Valley fault lie within the region of positive stress change contours. Along the Rainbow Mountain fault, however, there is a northeast trend of seismicity in an area where the static stresses where reduced. The mismatch between seismicity and regions of increased static stress changes may be a result of the poor epicentral location of some of the events which may have an error of 5 km.

## Discussion

The Rainbow Mountain earthquakes transferred a positive but relatively low stress increase onto the Fairview Peak fault compared to that transferred to the Dixie Valley fault. It is therefore puzzling that the Fairview Peak fault failed first. There are two possible explanations. First, the West Gate/Gold King faults, which received a stress increase of $0.7 \times 10^5$ Pa may have begun to slip before the Fairview Peak event and triggered the Fairview event. Although the time and focal mechanisms for the West Gate/Gold King events are undetermined, the faults are assumed to have ruptured with the Fairview Peak event [*Doser*, 1986]. Second, the order in which the Fairview Peak and Dixie Valley faults failed may have been controlled by the 1932, $M$=6.7, Cedar Mountain

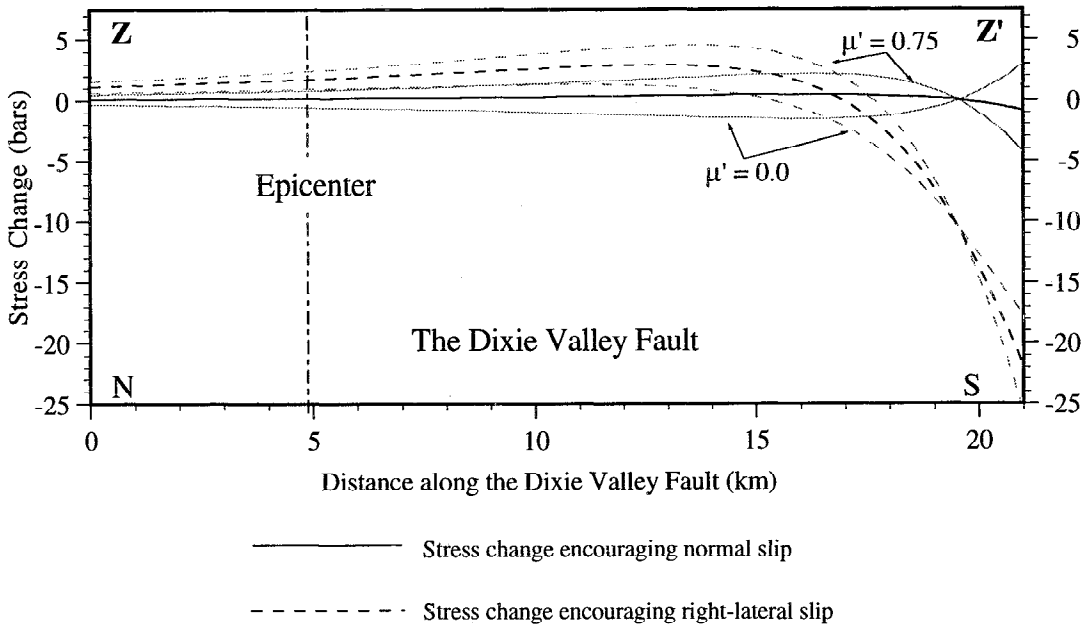


**Figure 8.** Stress resolved onto the Dixie Valley fault caused by the Rainbow Mountain, Fairview Peak, and West Gate/Gold King events.

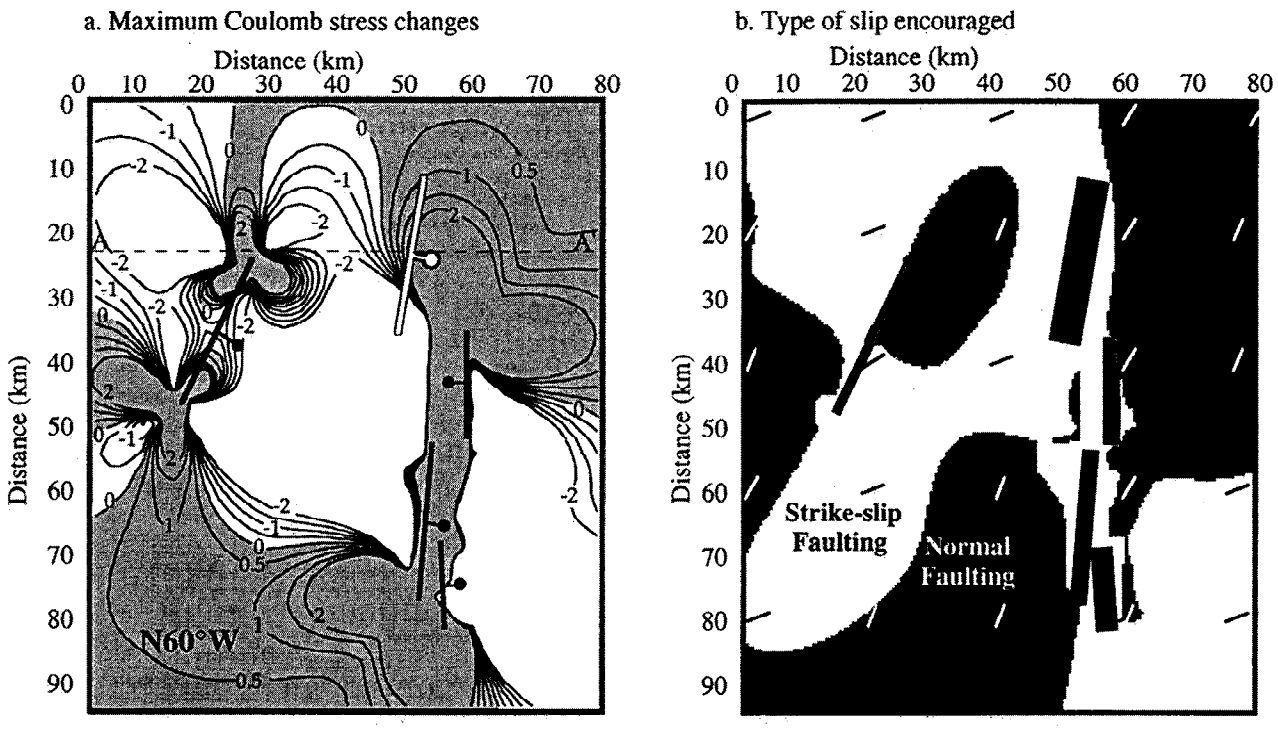


**Figure 9.** Coulomb stress change fields associated with slip on the Rainbow Mountain, Fairview Peak, and West Gate/Gold King faults; $\mu = 0.4$. Faults in black indicate those which have slipped, while those in white indicate those which have yet to fail. (a) The maximum Coulomb stress change fields. The stress changes are contoured at $0.5 \times 10^5$ Pa intervals. (b) Type of slip encouraged. Black areas show where stress changes encouraging normal faulting are greater than those encouraging strike-slip faulting. White areas show where stress changes encouraging strike-slip faulting were greatest.

earthquake. The Cedar Mountain earthquake (Figure 2) was one of almost pure strike-slip motion on a near vertical fault 60 km from the Fairview Peak fault [*Doser,* 1988]. That event increased the static stresses on the Fairview Peak fault by up to $0.17 \times 10^5$ Pa, while the stress increases on the Dixie Valley fault were less than $0.05 \times 10^5$ Pa. The Fairview Peak fault may therefore have been relatively closer to failure than the Dixie Valley fault. The stress increases on the Rainbow Mountain fault was less than $0.1 \times 10^5$ Pa. The 1915 $M$=6.9 Pleasant Valley earthquake, which occurred 90 km from the Dixie Valley epicenter (Figure 2), had a very small effect on the Dixie Valley and Fairview Peak faults. Both faults were discouraged from failing through normal faulting by stress changes of $0.03 \times 10^5$ Pa. Right-lateral slip was encouraged by stress changes of $0.08 \times 10^5$ Pa and $0.04 \times 10^5$ Pa on the Dixie Valley and Fairview Peak faults, respectively. At stress changes of $< 0.1 \times 10^5$ Pa, however, the correlation of seismicity and positive static stress changes is weak [*Reasenberg and Simpson,* 1994]. The effects of earthquakes 2 or 3 centuries ago are probably small compared to the effects of earthquakes this century. *Harris and Simpson* [1996] show that seismicity following the great $M$=7.8, 1857 Fort Tejon earthquake influenced the distribution of subsequent earthquakes for only 50 years. Thus, although there were other earthquakes in the area preceding the beginning of the historical record, their effects are probably small compared to earthquakes of this century.

The Rainbow Mountain events, although associated with the smallest amount of slip, appear to play an important role in the triggering of the Dixie Valley earthquake. The Dixie

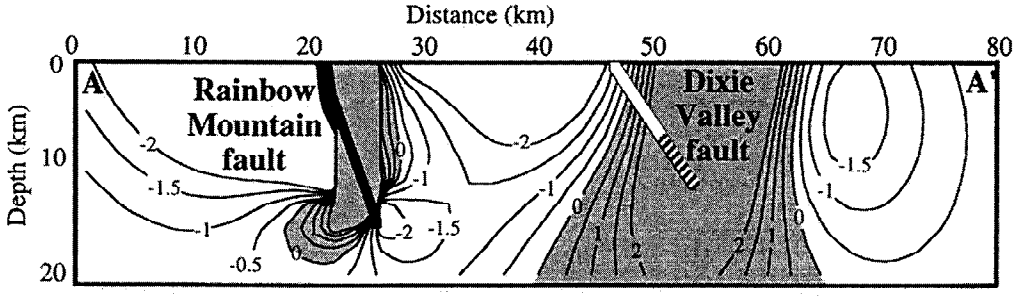


**Figure 10.** Variation in maximum Coulomb stress change with depth due to slip on all but the Dixie Valley faults along profile AA' (see Figure 9a). The stress changes are contoured at $0.5 \times 10^5$ Pa intervals. White fault line shows the geodetically inferred Dixie valley fault, the hashed extension shows the extension to the focal depth calculated by *Doser* [1986].

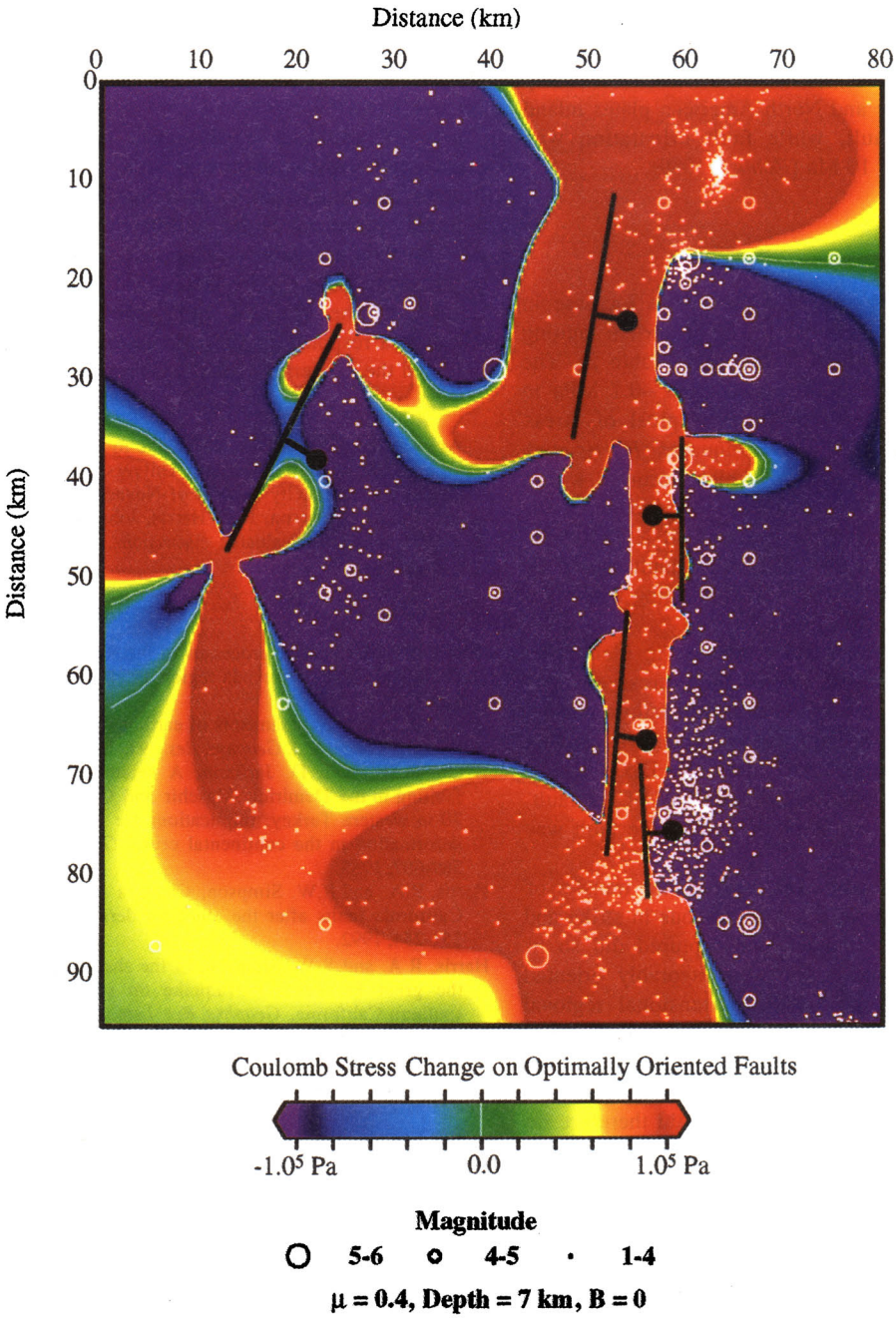


**Plate 1.** Regions of increased Coulomb stress caused by the 1954 sequence of earthquakes and aftershocks from December 16, 1954, to January 1, 1991.

Valley fault received a large stress increase from the Rainbow Mountain event because of the relative geometrical position of the faults, the orientation of the regional stress, and the right-lateral motion which occurred on the Rainbow Mountain fault. This combination of factors caused a lobe of static stress changes of 1 x $10^5$ Pa to fall in the region of the Dixie Valley fault. The stress changes which preceded rupture on the Dixie Valley fault encouraged failure through normal and right-lateral slip and were greatest at the northern end of the fault where rupture began [*Doser*, 1986].

Generally, about one fault depth away from the ruptured faults stresses are relaxed on optimally oriented faults (Plate 1). Stresses are increased however within 5 to 10 km of the rupture zones and at the fault end points. The combination of fault orientation and current regional stress field may explain the northeast-southwest trend of seismicity through the Central Nevada Seismic Zone. As is seen in Figures 6 and 9 and Plate 1, a lobe of high stress change tends to fall to the northeast and southwest of the faults, while lobes of negative stress change tend to fall to the northwest and southeast of the faults. The static stress changes therefore favor the propagation of seismicity to continue in a northeast or southwest direction on optimally oriented faults. This is a result of the northeasterly orientation of the faults in the Central Nevada Seismic Zone and the northwest orientation of the regional stress field. Seismicity along the western edge of the Basin and Range

province is therefore influenced by past and present tectonism since the current northwest orientation of the least principal stress is probably a result of the distribution of strike-slip motion between the Pacific and North American plates inland from the San Andreas fault, while fault orientation was determined between 17 and 10 Ma [*Zoback*, 1989].

## Conclusion

Each event in the 1954 sequence caused an increase in static stresses, encouraging right-lateral and/or normal faulting on some part of the faults which failed next (Table 2). The magnitude of the stress increases ranged from ~0.1 MPa to over 0.1 MPa (1 bar). These values are typical of stress changes which are thought to trigger earthquakes. *Harris et al.* [1995] found that M≥5.5 earthquakes which occurred within 1.5 years of a large event almost always occurred on fault planes which had received a stress increase of ≥ $1x10^5$ Pa. Also, the increase in stress along the Landers fault caused by four events in the region in the 24 years preceding that event was about $1x10^5$ Pa [*King et al.*, 1994].

These calculations also have some success in identifying the epicentral area of triggered events. The stress changes preceding the Fairview Peak event encouraged failure only at the northern end of the fault where the epicenter was located [*Doser*, 1986]. Stress changes preceding the Dixie Valley earthquake were greatest along the northern half of the fault, where rupture began, while the southern half of the fault was in effect clamped shut.

The 1954 sequence of earthquakes involved the transfer of stress between faults which were not continuous in strike and did not join at depth. The faults which ruptured did so in regions of static stress increases and were favorably oriented for dip-slip failure given the existing extensional regional stress regime. This suggests the northeast trending zone exists as a result of the orientation of preexisting faults and the current regional stress field. The current heightened seismicity within the zone and the trend of the zone could therefore be attributed to processes within the brittle crust and not solely to process in the lower crust such as a narrow zone of localized extension at depth as proposed by *Wallace* [1984].

Patterns of normal faulting events similar to the Fairview Peak-Dixie Valley events have been observed in other regions. In southwest Turkey, a region of continental extension similar to the Basin and Range province, three normal faulting events of $M_s$=5.9, 6.5, and 7.2 occurred within 100 km of each other in 1969 and 1970. The time intervals between the events were 5 days and 1 year. Similar to the Nevada sequence, the events occurred on faults that were not continuous in strike and oriented east-west in a north-south extensional regime [*Eyidogan and Jackson*, 1985]. In 1981, three earthquakes of $M_s$=6.7, 6.4, and 6.4 occurred in the easternmost part of the Gulf of Corinth [*Jackson et al.*, 1982]. The events occurred on normal faults within 30 km of each other. The first two events were separated by 2 hours and the second and third events were separated by 7 days. These faults were favorably oriented for failure in an extensional regime [*Hubert et al.*, 1996]. The Wasatch fault zone is a 370-km north-south trending fault zone in western Utah. There have been no earthquakes in the zone in historic time, but paleoseismological evidence suggests $M_s$=6.5 to 7 earthquakes repeatedly occur along it [*Schwartz and Coppersmith*, 1984]. It appears that most of the fault zone ruptured between 1000 and 500 years ago, suggesting that seismicity may have propagated through it in a manner similar to that occurring now in the Central Nevada Seismic Zone.

Normal faulting earthquakes accommodate regional extensional stresses within an area, and when a fault fails, stresses are transferred to some regions off it. If there are favorably oriented faults within the region of increased stresses, then a sequence of normal faulting earthquakes may be "triggered", such in Dixie Valley, southwest Turkey, Greece, or the Wasatch fault zone. Such sequences are therefore a response to the orientation of the regional stress field and the existence of faults favorably oriented for failure.

**Acknowledgments.** We would like to thank Martha Savage at the Center of Neotectonic Studies, University of Nevada, Reno, for supplying the seismicity records of Nevada. We would also like to thank George Thompson, Ruth Harris, John Caskey, Steve Jaumé and Steve Wesnousky for valuable discussions.

## REFERENCES

Doser, D.I., Earthquake processes in the Rainbow Mountain-Fairview Peak-Dixie Valley, Nevada region 1954-1959, *J. Geophys. Res., 91*, 12,572-12,586, 1986.

Doser, D.I., Source parameters of earthquakes in the Nevada Seismic Zone, 1915-1943, *J. Geophys. Res., 93*, 15,001-15,015, 1988.

Eyidogan, H., and D. Jackson, A seismological study of normal faulting in the Demirici, Alasehir and Gediz earthquakes of 1969-70 in western Turkey: Implications for the nature and geometry of deformation in the continental crust, *Geophys. J. R. Astr. Soc.*, *81*, 569-607, 1985.

Harris, R.A., and R.W. Simpson, Changes in static stress on southern California faults after the 1992 Landers earthquake, *Nature, 360*, 251-254, 1992.

Harris, R.A. and R.W. Simpson, In the shadow of 1857- the effect of the great Ft. Tejon earthquake on subsequent earthquakes in southern California, *Geophys. Res. Lett., 23*, 229-232, 1996.

Harris, R.A., R.W. Simpson, and P. A. Reasenberg, Influence of static stress changes on earthquake locations in southern California, *Nature, 375*, 221-224, 1995.

Hodgkinson, K.M., R.S. Stein, and G. Marshall, Geometry of the 1954 Fairview Peak-Dixie Valley earthquake sequence from a joint inversion of leveling and triangulation data, *J. Geophys. Res., this issue*.

Hubert, A., G.C.P. King, R. Armijo, and B., Meyer, Fault reactivation, stress interaction and rupture propagation in the 1981 Corinth sequence, *Earth Planet. Sci. Lett.*, in press, 1996.

Jackson, J.A., J. Gagnepain, G. Houseman, G.C.P. King, P. Papadimitriou, C. Soufleris and J. Virieux, Seismicity, normal faulting, and the geomorphological development of the Gulf of Corinth (Greece): The Corinth earthquakes of February and March 1981, *Earth Planet. Sci. Lett., 57*, 377-397, 1982.

Jaumé, S. C., and L. R. Sykes, Change in the state of stress on the southern San Andreas fault resulting from the California earthquake sequence of April to June, 1992, *Science, 258*, 1325-1328, 1992.

King, G.C.P., R.S. Stein, and J. Lin, Static stress changes and the triggering of earthquakes, *Bull. Seismol. Soc. Am., 84*, 935-953, 1994.

Okada, Y., Internal deformation due to shear and tensile faults in a half-space, *Bull. Seismol. Soc. Am., 82*, 1018-1040, 1992.

Okaya, D.A., and G.A. Thompson, Geometry of Cenozoic extensional faulting: Dixie Valley, Nevada, *Tectonophysics, 4*, 107-125, 1985.

Reasenberg, P.A., and R.W. Simpson, Response of regional seismicity to the static stress change produced by the Loma Prieta earthquake, *Science, 255*, 1687-1690, 1992.

Rice, J.R., Fault stress states, pore pressure distributions, and the weakness of the San Andreas fault, in *Fault Mechanics and Transport Properties of Rock*, edited by B. Evans and T.-F. Wong, pp.475-503, Academic, San Diego, Calif., 1992.

Roeloffs, E.A., Fault stability changes induced beneath a reservoir with cyclic variations in water level, *J. Geophys. Res. 93*, 2107-2124, 1988.

Savage, J.C., M. Lisowski, J.L. Svarc, and W.K. Gross, Strain accumulation across the central Nevada seismic zone, 1973-1994, *J. Geophys. Res., 100,* 20-257-20269, 1995.

Scholz, C.H., *The Mechanics of Earthquakes and Faulting*, 439 pp., Cambridge Univ., New York, 1990.

Schwartz, D.P., and K.J. Coppersmith, Fault behavior and characteristic earthquakes; Examples from the Wasatch and San Andreas fault zones, *J. Geophys. Res., 89,* 5681-5698, 1984.

Simpson, R.W., and P.A. Reasenberg, Earthquake-induced static-stress changes on central California faults, in *The Loma Prieta, California, earthquake of October 17, 1989; Tectonic Processes and Models*, edited by R. W. Simpson, *U.S. Geol. Surv. Prof. Pap., P1550-F,* F1-F131, 1994.

Slemmons, D.B., Geological effects of the Dixie Valley-Fairview Peak, Nevada, earthquakes of December 16, 1954, *Bull. Seismol. Soc. Am., 47,* 353-376, 1957.

Stein, R.S., G.C.P. King, and J. Lin, Change in failure stress on the southern San Andreas fault system caused by the 1992 Magnitude = 7.4 Landers earthquake, *Science, 258,* 1328-1332, 1992.

Stein, R. S., and M. Lisowski, The 1979 Homestead Valley earthquake sequence, California: Control of aftershocks and postseismic deformation, *J. Geophys. Res. 88,* 6477-6490, 1983.

Turcotte, D.L. and G. Schurbert, *Geodynamics, Applications of continuum physics to geological problems*, John Wiley & Sons Inc., New York, pp 450, 1982.

Wallace, R.E., Patterns and timing of late Quaternary faulting in the Great Basin Province and relation to some tectonic features, *J Geophys. Res., 89,* 5763-5769, 1984.

Ward, S., Pacific-North America plate motions: New results from Very Long Baseline Interferometry, *J. Geophys. Res., 95,* 21,965-21,981, 1990.

Zoback, M.L., State of stress and deformation in the northern Basin and Range Province, *J. Geophys. Res., 94,* 7105-7128, 1989.

K.M. Hodgkinson and R.S. Stein, U.S. Geological Survey, MS 977, 345 Middlefield Road, Menlo Park, Ca 94025. (email: kathleen@andreas.wr.usgs.gov; rstein@usgs.gov; ).

G.C.P. King, Institut de Physique du Globe de Paris, Tectonique Lab, 4 Place Jussieu, 75252 Paris Cedex, France.

(Received December 1 1995; revised April 19, 1996; accepted April 25, 1996.)